

and Flame Elsevier Editorial System(tm) for Combustion
Manuscript Draft

Manuscript Number: CNF-D-16-00540R3

Title: Outlier analysis for a silicon nanoparticle population balance model

Article Type: Accepted Paper

Keywords: Silicon; nanoparticles; population balance; regression influence diagnostics

Corresponding Author: Professor Markus Kraft,

Corresponding Author's Institution: University of Cambridge

First Author: Sebastian Mosbach, PhD

Order of Authors: Sebastian Mosbach, PhD; William J Menz; Markus Kraft

Manuscript Region of Origin: UNITED KINGDOM

1
2
3
4
5
6
7
8
9
10
11
12
13
14
15
16
17
18
19
20
21
22
23
24
25
26
27
28
29
30
31
32
33
34
35
36
37
38
39
40
41
42
43
44
45
46
47
48
49
50
51
52
53
54
55
56
57
58
59
60
61
62
63
64
65

Outlier analysis for a silicon nanoparticle population balance model

Sebastian Mosbach^a, William J. Menz^a, Markus Kraft^{a,b,*}

^a*Department of Chemical Engineering and Biotechnology, University of Cambridge
New Museums Site, Pembroke Street, Cambridge CB2 3RA, United Kingdom*

^b*School of Chemical and Biomedical Engineering, Nanyang Technological University
62 Nanyang Drive, Singapore 637459, Singapore*

Abstract

We assess the impact of individual experimental observations on a multivariate population balance model for the formation of silicon nanoparticles from the thermal decomposition of silane by means of basic regression influence diagnostics. The nanoparticle model is closely related to one which has been used to simulate soot formation in flames and includes morphological and compositional details which allow representation of primary particles within aggregates, and of coagulation, surface growth, and sintering processes. Predicted particle size distributions are optimised against 19 experiments across ranges of initial temperature, pressure, residence time, and initial silane mass fraction. The influence of each experimental observation on the model parameter estimates is then quantified using the Cook distance and DFBETA measures. Seven model parameters are included in the analysis, with five Arrhenius pre-exponential factors in the gas-phase kinetic rate expressions, and two kinetic rate constants in the population balance model. The analysis

*Corresponding author
Email address: mk306@cam.ac.uk (Markus Kraft)

1
2
3
4
5
6
7
8
9 highlights certain experimental conditions and kinetic parameters which war-
10 rant closer inspection due to large influence, thus providing clues as to which
11 aspects of the model require improvement. We find the insights provided can
12 be useful for future model development and planning of experiments.
13
14

15
16 *Keywords:* Silicon, nanoparticles, population balance, regression influence
17 diagnostics
18
19

20 21 22 **1. Introduction** 23

24
25 Gas-phase synthesis in hot-wall reactors is a common way in which sili-
26 con nanoparticles are manufactured. Shock-tubes are another set-up in which
27 especially the early phase of formation of these particles can be studied. Typ-
28 ically, these synthesis processes begin with silane (SiH_4) as a precursor, which
29 is transformed into the eventual nanoparticle product at high temperatures.
30 A variety of models have been proposed to describe this transformation [1].
31 These models usually contain unknown or low-confidence (kinetic) parame-
32 ters with large uncertainties associated to them. Systematic parameter esti-
33 mation techniques can then be employed to arrive at better values for these
34 quantities, based on available experimental data. One of the most elementary
35 parameter estimation methods is least-squares optimisation, *i.e.* minimis-
36 ing the distance between experimental observations and model prediction as
37 measured by a sum-of-squares objective function. The result of such an op-
38 timisation is a set of values, called ('best') estimates, for the selected model
39 parameters. Not all experimental data points may equally inform the optimal
40 value of the parameters, though – different parameters may be determined
41 to a varying extent by different observations. In order to assess which ex-
42
43
44
45
46
47
48
49
50
51
52
53
54
55
56
57
58
59
60
61
62
63
64
65

1
2
3
4
5
6
7
8
9
10
11
12
13
14
15
16
17
18
19
20
21
22
23
24
25
26
27
28
29
30
31
32
33
34
35
36
37
38
39
40
41
42
43
44
45
46
47
48
49
50
51
52
53
54
55
56
57
58
59
60
61
62
63
64
65

periments are the most relevant in the optimisation, one can conduct what may be called an omission-based regression influence analysis [2]: Firstly, optimise the model against the full data set, and then repeat the optimisation with one of the data points removed, for each of the data points. Based on the difference between the parameter estimates of the full optimisation and the optimisations with an omitted data point, it is then possible to quantify the influence of individual observations on the model overall or on individual parameters. Several such measures have been proposed [3, 4], the most widely-used one being Cook’s distance [5], and applied to detect influential data points, high-leverage points, and statistical outliers [6, 7].

An alternative approach to quantifying influence of experimental observations is uncertainty propagation [8], part of which is concerned with how experimental measurement errors propagate into model parameters and responses. Some of these methods allow calculating the relative contribution of each data point (and its error bar) to the uncertainty in each of the parameters. In particular, the Data Collaboration framework [9] exploits the pairwise consistency of data set units to identify outliers.

Yet another approach, called perturbation of the optimum, has been developed for constrained optimisation [10, p. 34] and unconstrained least-squares optimisation [11], which has found application in chemical kinetics [12, 13, 2]. These methods allow calculating sensitivities of parameter estimates with respect to any other quantity in the objective function (or constraints), including in particular experimental data.

The purpose of this paper is to conduct an omission-based outlier analysis of a selection of experimental data for silicon nanoparticles produced from

1
2
3
4
5
6
7
8
9 a silane precursor in hot-wall flow reactors and shock tubes which are mod-
10 elled using a detailed population balance model. A main aim is to identify
11 those experimental conditions which are the most challenging for the model.
12 We apply a technique established in the field of regression influence diag-
13 nostics to quantify the influence of individual experimental observations on
14 kinetic parameter estimates for this purpose. We determine the influence of
15 the measurements on estimates of some Arrhenius pre-exponential factors in
16 the gas-phase kinetic mechanism as well as the population balance model for
17 the particle phase. Using a threshold for the influence values, specific mea-
18 surements are then highlighted for further analysis, providing further insight
19 into the model and potential improvements, as well as suggestions for future
20 experiments.
21
22
23
24
25
26
27
28
29
30
31

32 33 **2. Background** 34

35
36 We firstly describe the model, provide some background on omission-
37 based regression influence diagnostics, and how it can be used to identify
38 outliers.
39
40

41 42 *2.1. Population balance model for silicon nanoparticle formation* 43

44
45 We briefly summarise the main features of the model here. Full details can
46 be found in [1], and further in [16, 17, 18, 19, 20], noting that a closely related
47 model has been applied to soot formation in flames (see for example [21] and
48 references therein). It consists of two main parts, a gas-phase model, and a
49 particulate phase model.
50
51
52
53
54
55
56
57
58

1
2
3
4
5
6
7
8
9
10
11
12
13
14
15
16
17
18
19
20
21
22
23
24
25
26
27
28
29
30
31
32
33
34
35
36
37
38
39
40
41
42
43
44
45
46
47
48
49
50
51
52
53
54
55
56
57
58
59
60
61
62
63
64
65

Table 1: The gas-phase kinetic mechanism. Values in bold correspond to parameters chosen for the influence analysis. Units for the Arrhenius pre-exponential factors are cm, mol, and s.

Idx.	Reaction	A	β [-]	E [kcal/mol]	Ref.
1	$\text{SiH}_4 (+\text{M}) \rightleftharpoons \text{SiH}_2 + \text{H}_2 (+\text{M})$	3.12×10^9	1.7	54.71	[14]
	Low pressure limit:	3.96×10^{12}	0	45.10	[15, 1] ¹
2	$\text{Si}_2\text{H}_6 (+\text{M}) \rightleftharpoons \text{SiH}_4 + \text{SiH}_2 (+\text{M})$	1.81×10^{10}	1.7	50.20	[14]
	Low pressure limit:	5.09×10^{53}	-10.37	56.03	[14]
3	$\text{Si}_2\text{H}_6 (+\text{M}) \rightleftharpoons \text{Si}_2\text{H}_4\text{B} + \text{H}_2 (+\text{M})$	9.09×10^9	1.8	54.20	[14]
	Low pressure limit:	7.79×10^{40}	-7.77	59.02	[14, 1] ²
4	$\text{Si}_3\text{H}_8 (+\text{M}) \rightleftharpoons \text{SiH}_2 + \text{Si}_2\text{H}_6 (+\text{M})$	6.97×10^{12}	1.0	52.68	[14]
	Low pressure limit:	1.73×10^{69}	-15.07	60.49	[14]
5	$\text{Si}_3\text{H}_8 (+\text{M}) \rightleftharpoons \text{Si}_2\text{H}_4\text{B} + \text{SiH}_4 (+\text{M})$	3.73×10^{12}	1.0	50.85	[14]
	Low pressure limit:	4.36×10^{76}	-17.26	59.30	[14]
6	$\text{Si}_2\text{H}_4\text{B} (+\text{M}) \rightleftharpoons \text{Si}_2\text{H}_4\text{A} (+\text{M})$	2.54×10^{13}	-0.2	5.38	[14]
	Low pressure limit:	1.10×10^{33}	-5.76	9.15	[14]
7	$\text{Si}_2\text{H}_4\text{B} + \text{H}_2 \rightleftharpoons \text{SiH}_4 + \text{SiH}_2$	9.41×10^{13}	0	4.09	[14]
	Reverse coefficients:	9.43×10^{10}	1.1	5.79	[14]
8	$\text{Si}_2\text{H}_4\text{B} + \text{SiH}_4 \rightleftharpoons \text{Si}_2\text{H}_6 + \text{SiH}_2$	1.73×10^{14}	0.4	8.90	[14]
	Reverse coefficients:	2.65×10^{15}	0.1	8.47	[14]

¹ A is from [1], β and E are from [15]. ² A is from [1], β and E are from [14].

1
2
3
4
5
6
7
8
9
10
11
12
13
14
15
16
17
18
19
20
21
22
23
24
25
26
27
28
29
30
31
32
33
34
35
36
37
38
39
40
41
42
43
44
45
46
47
48
49
50
51
52
53
54
55
56
57
58
59
60
61
62
63
64
65

2.1.1. Gas phase

The gas-phase chemical kinetic reaction mechanism used is a modified version of the one proposed by [14], and is summarised in Table 1. Two isomers of Si_2H_4 are included: silene, *i.e.* H_2SiSiH_2 , denoted by the suffix “A”, and silylene, *i.e.* HSiSiH_3 , denoted by the suffix “B”. The first six reactions are third-body reactions whose pressure-dependence is given in Lindemann fall-off form. More details can be found in [1].

2.1.2. Particulate phase

The particle phase is described by a detailed, high-dimensional population balance model [1] covering aggregate morphology and chemical composition. In this model, each nanoparticle is represented as a list of primary particles, together with a (triangular) matrix, called connectivity matrix, each entry of which represents the common surface area for the corresponding pair of primary particles. For each primary particle, the number of silicon and the number of hydrogen atoms are stored. From this particle representation, beyond elementary properties like mass and chemical composition, several quantities of interest can be derived. These include for example, with some additional assumptions, collision and mobility diameter of aggregates, surface area, and sintering level.

The following processes which create or transform particles, or account for interaction of the particles with the gas phase, are represented in the model:

Inception: Any two molecules of any of the three species SiH_2 , $\text{Si}_2\text{H}_4\text{A}$, and $\text{Si}_2\text{H}_4\text{B}$ can collide to (irreversibly) form a new particle, which is assumed to consist of a single, spherical primary whose diameter follows directly from

1
2
3
4
5
6
7
8
9 its mass, *i.e.* numbers of atoms. The rate at which this happens is as-
10 sumed to be non-zero only if the diameter of the resulting particle exceeds a
11 temperature- and pressure-dependent critical nucleus diameter. If the latter
12 is the case, the inception rate is proportional to the product of the concentra-
13 tions of the collision partners and the transition regime coagulation kernel.
14 More details can be found in [1] and [16].
15
16
17
18
19

20 *Condensation:* An existing particle can grow through (barrier-free) de-
21 position of SiH_2 , $\text{Si}_2\text{H}_4\text{A}$, or $\text{Si}_2\text{H}_4\text{B}$ molecules from the gas phase onto its
22 surface. It is assumed that the collision efficiency, *i.e.* the probability of
23 sticking, is unity. The rate is given by a free-molecular collision kernel.
24
25
26
27

28 *Surface reaction:* Apart from simply condensing, gas-phase species can
29 also react heterogeneously on the particle surface. Specifically, silanes (SiH_4 ,
30 Si_2H_6 , and Si_3H_8) can be integrated into the particle, with each step releasing
31 one, two, and three molecules of hydrogen, respectively. The rate is propor-
32 tional to the particle surface area and an Arrhenius expression with non-zero
33 activation energy. Rounding of adjacent primary particles caused by this
34 process is also taken into account.
35
36
37
38
39
40

41 *Hydrogen release:* In order to attain a stable crystal structure, particles
42 need to release some of the hydrogen acquired through each of the above
43 processes. The rate of desorption is proportional to an Arrhenius expression
44 and the coverage of hydrogen on the particle surface, which is approximated
45 by the ratio of hydrogen to silicon atoms within the particle. It is assumed
46 that the sintering level of adjacent primaries is unaffected by this process,
47 *i.e.* the connectivity matrix remains unchanged.
48
49
50
51
52
53

54 *Coagulation:* Two particles can collide and stick to each other at their
55
56
57
58
59
60
61
62
63
64
65

point of contact. The rate is given by transition regime coagulation kernel, which is the harmonic mean of the slip-flow and free-molecular kernels. The transition kernel is valid across a wide range of Knudsen numbers, and thus wide ranges of pressures and particle sizes (see [19] and [22] for more details).

Sintering: The sintering of any pair of adjacent primary particles is modelled by an exponential decay of the excess of the joint surface area of the primaries compared to the surface area of their equivalent sphere. In other words, the corresponding entry in the connectivity matrix decreases exponentially towards the equivalent spherical area of the primary particle pair.

2.2. Omission-based regression influence diagnostics

2.2.1. Parameter estimation

Given a set of N experimental observations η_n^{exp} , with $n = 1, \dots, N$. For example, these could be, as in this work, means or modes of the particle size distribution at given temperatures and pressures. Assuming we have a model which depends on a vector ϑ of P model parameters, we denote its response for the conditions of the n^{th} experiment by $\eta_n(\vartheta)$. For simplicity, we restrict ourselves in this work to a single response, but the generalisation of all that follows to multiple responses is straightforward.

In order to quantify agreement between experiment and model, a measure of the distance between the model response and experimental results needs to be defined. We use the ordinary least-squares objective function

$$\Phi(\vartheta) := \sum_{n=1}^N [\eta_n(\vartheta) - \eta_n^{\text{exp}}]^2 \quad (1)$$

for this purpose. The term ‘ordinary’ refers to the fact that the covariance matrix of the responses is the unity matrix, *i.e.* the responses are assumed

1
2
3
4
5
6
7
8
9 to be uncorrelated and are subject to the same or very similar uncertainties,
10 meaning all the terms in the sum are equally weighted.

11 The vector $\hat{\vartheta}$ of parameter values which are optimal with respect to the
12 objective function can be obtained by minimising (1):
13
14

$$15 \quad \hat{\vartheta} := \underset{\vartheta}{\operatorname{argmin}} \Phi(\vartheta) \quad (2)$$

16
17 The best estimate of the model responses is then defined as $\hat{\eta} := \eta(\hat{\vartheta})$.
18
19

20 2.2.2. Influence measures

21 The basic idea underlying omission-based regression influence diagnostics
22 is to analyse the effect of deleting a single observation from the considered
23 set of data. In the following, we use a subscript “ $-i$ ” to denote quantities
24 based on the data set with the i^{th} observation removed. In particular, the
25 objective function (1) becomes
26
27

$$28 \quad \Phi_{-i}(\vartheta) := \sum_{n=1, \dots, i-1, i+1, \dots, N} [\eta_n(\vartheta) - \eta_n^{\text{exp}}]^2, \quad (3)$$

29 with the corresponding best parameter estimate
30
31

$$32 \quad \hat{\vartheta}_{-i} := \underset{\vartheta}{\operatorname{argmin}} \Phi_{-i}(\vartheta) \quad (4)$$

33 and response estimate $\hat{\eta}_{-i} := \eta(\hat{\vartheta}_{-i})$.
34
35

36 There are numerous ways of assessing how the optimum, *i.e.* the best
37 estimate of the parameters, is affected by removing a data point [7]. The
38 most elementary statistic is obtained by considering the difference between
39 the best estimate of the parameters and the best estimate with the i^{th} data
40 point removed:
41
42

$$43 \quad D_{ij}^* := \hat{\vartheta}_j - \hat{\vartheta}_{-i,j}, \quad (5)$$

1
2
3
4
5
6
7
8
9 where $\hat{\vartheta}_{-i,j}$ is the value of the j^{th} parameter obtained from the optimisation
10 with the i^{th} experiment omitted. In the literature this is usually referred to
11 as DFBETA $_i$ [23, p. 13].
12
13

14 We note that such an analysis requires $\hat{\vartheta}_{-i}$ to be calculated for all $i =$
15 $1, \dots, N$, each requiring one optimisation. This can become computation-
16 ally prohibitively expensive if the model itself is expensive or there are many
17 experimental observations. If the considered model is linear, at least approx-
18 imately, then it is possible to derive a formula which allows calculating the
19 entire set of D_{ij}^* based on only a single optimisation [2]. This, however, is
20 not an option if the model responses are strongly non-linear or are subject
21 to numerical or statistical noise. The model considered in this work is by
22 nature a stochastic model and its responses do exhibit non-negligible noise.
23
24
25
26
27
28
29
30
31

32 In order to compare or rank different parameters against each other with
33 respect to their influence, due to different physical dimensions and/or or-
34 ders of magnitude, it is essential to consider non-dimensionalised diagnos-
35 tic measures. Belsley et al. [23, p. 13] recommend to normalise by the
36 square root of an estimate of the variance of each parameter (with the i^{th}
37 data point removed). This allows assessing the influence of data points on
38 each parameter in relation to their uncertainty. Specifically, they propose
39 to measure the influence of the i^{th} experiment upon the j^{th} parameter using
40 DFBETAS $_{ij} := D_{ij}^*/(\text{Var } \hat{\vartheta}_j)^{1/2}$ (see also [24]), where $\text{Var } \hat{\vartheta}_j$ refers to the vari-
41 ance of the j^{th} parameter. In some situations, the parameter variance may
42 not be readily available, such as in this work where we directly optimise the
43 model while progressively excluding experiments. Hence, we simply use here
44 parameters which are normalised by (logarithmically) mapping them to the
45
46
47
48
49
50
51
52
53
54
55
56
57
58
59
60
61
62
63
64
65

interval $[-1, 1]$.

Cook's distance [5], one of the most widely-used influence diagnostics, can be a useful tool for assessing the influence of an experimental data point during an optimisation. In the special case we consider in this work, *i.e.* that of uncorrelated responses with similar uncertainty, it can be defined as [7]

$$C_i := \frac{\sum_{n=1}^N [\hat{\eta}_n - \hat{\eta}_{-i,n}]^2}{Ps^2}, \quad (6)$$

where $\hat{\eta}_{-i,n}$ is the value of the model response for the conditions of the n^{th} experiment obtained using the best parameter value estimates determined through optimisation with the i^{th} observation omitted (*i.e.* $\hat{\vartheta}_{-i}$), and where s^2 is an estimate of the mean square error, given by

$$s^2 = \frac{1}{N - P} \sum_{n=1}^N (\eta_n^{\text{exp}} - \hat{\eta}_n)^2. \quad (7)$$

Large values of Cook's distance C_i occur if deleting case i causes large differences in the parameter estimates.

The motivation for definition (6) stems from the notion of joint confidence regions for the parameters. Joint $100(1 - \alpha)\%$ confidence ellipsoids for the model responses can be defined as

$$(\hat{\eta} - \eta)^\top \Sigma^{-1} (\hat{\eta} - \eta) \leq Ps^2 F(P, N - P, 1 - \alpha), \quad (8)$$

with s given by (7), and $F(P, N - P, 1 - \alpha)$ the $1 - \alpha$ point of the F -distribution (consult [25, pp. 94 & 108] and [26] for more details). Σ is the covariance matrix of the responses. Cook introduced his original measure [5, 27] for ordinary least squares, *i.e.* unity covariance matrix, and later generalised it to weighted least squares [3, p. 209]. As mentioned above, if the responses

1
2
3
4
5
6
7
8
9 are uncorrelated, of equal dimension, and of similar order of magnitude and
10 uncertainty, Σ can be assumed to be the unit matrix.

11
12
13 Definition (6), like (5), involves one optimisation per experimental data
14 point. As mentioned above, in situations where this is too computationally
15 expensive, there may be the option of conducting a linearised analysis. For
16 linear models, one can derive an expression for Cook's distance (6) which
17 requires only a single regression for all observations. Whether or not a linear
18 approximation is appropriate can be decided for example by means of local
19 curvature [28, 29], but this is beyond the scope of the paper.

20
21
22 It is noted that Cook's distance measures only the *overall* influence of an
23 observation, in contrast to (5), which assesses parameters individually. More
24 generally, while in this work we consider the influence of single observations
25 only on either single parameters or the model as a whole, this can be gen-
26 eralised to the influence of subsets of observations on subsets of parameters
27 in the model (see for example [24, 7]). As the original notions, however,
28 the measures tend to be applicable to linear models only, and may require
29 additional regressions.

30
31
32 It is furthermore noted that, unlike (5), the Cook distance (6) is dimen-
33 sionless by definition – a necessary property in order to achieve a generic
34 classification of data points.

35
36
37 In a wider context, recall that a more traditional way to examine the
38 influence of a data point on parameter estimates would be to conduct a sen-
39 sitivity analysis of the best estimates with respect to the measured data [12],
40 also known as perturbation of the optimum [30] (see also [2]). That is, con-
41 sider $\partial\hat{\theta}_j/\partial\eta_n^{\text{exp}}$, with (2) and (1). However, approximating such derivatives
42
43
44
45
46
47
48
49
50
51
52
53
54
55
56
57
58
59
60
61
62
63
64
65

1
2
3
4
5
6
7
8
9 by finite differences is problematic for stochastic, or otherwise noisy models,
10 such as in this application, as mentioned above. Additionally, omitting a
11 data point is not local in the sense that it causes a finite step-change in the
12 objective function rather than a small continuous change resulting from a
13 small perturbation of the data point, as is implied by the use of derivatives
14 in a sensitivity analysis.
15
16
17
18
19

20 21 *2.2.3. Outlier detection*

22
23 One way of identifying potential outliers is by means of a threshold: A
24 data point is deemed to require further attention if the corresponding value of
25 the chosen diagnostic measure exceeds the threshold. Naturally, the choice of
26 any such threshold is ultimately arbitrary, which is reflected in the fact that
27 a range of them has been suggested in the literature. For example, Bollen
28 and Jackman [31] propose
29
30
31
32
33
34

$$35 \quad C_i \geq 4/N. \quad (9)$$

36
37 This threshold is very conservative in the sense that it tends to highlight too
38 many points as outliers. On the other hand, Cook and Weisberg [32, p. 345]
39 suggest
40
41
42

$$43 \quad C_i \geq 1, \quad (10)$$

44
45 *i.e.* approximately the median of the F distribution with P and $N - P$
46 degrees of freedom (see Eqn. (8)). Irrespective of which value is chosen, it
47 needs to be emphasised that this method can give only a rough indication,
48 which should be interpreted merely as a suggestion of which data points
49 warrant closer investigation. The main reason for this is that the method does
50 not automatically distinguish between errors and highly influential points
51
52
53
54
55
56
57
58

1
2
3
4
5
6
7
8
9 which potentially point towards genuine model improvements. Therefore,
10 highlighted points should not necessarily be excluded from the analysis, as
11 one may lose valuable information. Furthermore, whether or not a data
12 point is deemed an ‘outlier’ by this method, is by definition dependent on
13 the chosen model. That is, a data point labelled an outlier with respect to
14 one model, may or may not appear as an outlier with respect to another
15 (possibly better) model. As there is no consensus in the literature as to
16 which cut-off should be used, in this work we consider both (9) and (10).
17
18
19
20
21
22
23
24

25 **3. Experimental data**

26
27
28 As in previous work [1, 20], a total of nineteen experimental data points
29 were selected from six different studies, spanning a range of process condi-
30 tions and reactor configurations. Reactor types include hot-wall flow reactors
31 and a shock tube, for each of which different temperatures, pressures, res-
32 idence times, and initial silane mole fractions are covered. The particular
33 selection of studies, an overview of which is given in Table 2, was motivated
34 by covering a range of conditions. This choice is, however, arbitrary amongst
35 large amounts of literature (too much to review here comprehensively), which
36 include further works on hot-wall reactors [39, 40, 41, 42], microwave reac-
37 tors [43, 44, 45], and plasma reactors [46, 47], to name but a few.
38
39
40
41
42
43
44
45
46
47

48 The study of Körmer et al. [33] is focused on synthesising silicon nanopar-
49 ticles with narrow size distributions in a hot-wall flow reactor. In this setup,
50 it turns out that most of the precursor is lost to deposits on the reactor wall,
51 and therefore the initial composition is adjusted to account for this particle
52 deposition [48]. As in [49], an initial silane mass of about 6×10^{-5} kg/m³ is
53
54
55
56
57
58
59
60
61
62
63
64
65

Table 2: Experimental data sets with process conditions used to model them. X_{SiH_4} denotes the initial silane mole fraction, and τ denotes the residence time.

Idx.	Reference	Reactor type	Bath gas	X_{SiH_4} [%]	T [K]	P [kPa]	τ [ms]	d type	μ type	μ_i^{exp} [nm]
1				4.0	873-1373		80		Mode	26.7
2				4.0	873-1373		192		Mean	26.0
3				12.0	873-1373		192		Mean	38.0
4	Körmer <i>et al.</i> [33]	Hot-wall flow reactor	Ar	12.8	873-1373		80		Mode	31.0
5				2.0	873-1373	2.5	80	d_{pri}	Mode	41.0
6				8.0	873-1373		80		Mode	24.0
7				4.0	873-1373		420		Mode	32.5
8				4.0	673-1173		420		Mode	21.2
9				4.0	773-1273		420		Mode	28.5
10	Frenklach <i>et al.</i> [34]	Shock tube	Ar		1089		2.6			11.0
11				3.3	1320	49	2.1	d_{pri}	Mode	11.0
12					1580		1.8			15.0
13	Wu <i>et al.</i> [35]	Hot-wall flow reactor	N ₂	1.0	770-1520	101	1000	d_{mob}	Mode	127
14	Flint <i>et al.</i> [36]	Laser- driven flow reactor	Ar	21.4	923-1270		5.2			43.4
15				9.0	1023-1483	20	18	d_{pri}	Mean	55.4
16				0.6	1023-1400		53			23.0
17	Nguyen and Flagan [37]	Hot-wall flow reactor	N ₂	0.1	770-1080	101	900	d_{mob}	Mode	89.0
18				0.04						
19	Onischuk <i>et al.</i> [38]	Hot-wall flow reactor	Ar	5.0	853	39	870	d_{pri}	Mean	52.0

assumed. The amount of mass expected for a partial pressure of 1 mbar of silane at 1024 K is about 3.8×10^{-4} kg/m³ indicating that only about 16% of the precursor are available to form particles. The initial silane fractions listed in Table 2 for this data subset are adjusted accordingly for our simulations.

The Flint *et al.* [36] data refers to their cases 630*S*, 631*S*, and 654*S*, respectively. The experiment is described in detail in [50, 51, 52], including how to convert flow rates into residence times and initial compositions.

1
2
3
4
5
6
7
8
9 Further work from the same group includes [53, 54].
10
11

12 4. Results and discussion 13 14

15 Both reactor types occurring in the set of experiments (Table 2), *i.e.*
16 flow reactor and shock tube, are modelled as homogenous batch reactors.
17 The shock tube is modelled as a constant temperature, constant pressure
18 reactor. For the flow reactors, plug-flow is assumed, and the experimentally
19 measured temperature profile, where available, is imposed. In case 19 [38],
20 no temperature profile is available, so a constant temperature is assumed,
21 and the residence time given refers to the approximate time spent in the
22 ‘hot-zone’, *i.e.* at that temperature.
23
24
25
26
27
28
29

30 As software to carry out the necessary optimisations, we use the Model
31 Development Suite (MoDS) [55] – a software tool for conducting various
32 generic tasks to develop black-box models. Such tasks include parame-
33 ter estimation and uncertainty quantification [56], Design of Experiments
34 (DoE) [57], and global sensitivity analysis [20].
35
36
37
38
39

40 Each optimisation involved in the Cook distance and DFBETA analysis is
41 performed in two stages: Firstly, a quasi-random global search is conducted
42 using Sobol low-discrepancy sequences [58]. Secondly, starting from the best
43 point identified in the first stage, a local optimisation is carried out using
44 the Simultaneous Perturbation Stochastic Approximation (SPSA) [59, 60]
45 algorithm. The SPSA method estimates the local gradient based on only
46 two objective function evaluations, and can be shown to obey the traditional
47 gradient descent *on average*. It is designed for problems where stochastic
48 noise is present. The motivation for the first stage is to avoid becoming
49
50
51
52
53
54
55
56
57
58
59
60
61
62
63
64
65

trapped in local minima or valleys on the objective function surface, which could happen with a method purely based on the local gradient. Chemical kinetic objective functions are widely reported to exhibit a complex, highly structured surface with multiple local minima and/or valleys (see for example [26]). Regarding the second stage, the reason for not choosing a more conventional method utilising the local Jacobi matrix or Hessian is the stochastic noise in the model response. While the procedure adopted here cannot guarantee to find the global minimum, based on previous experience [56], a low-lying minimum can be found at a manageable computational expense. On an objective function surface with multiple local minima, there is then of course the risk of selecting the ‘wrong’ optimum, *i.e.* not the global one. Any conclusions derived from perturbations such as those induced by omission of data points may change depending on the chosen minimum and the local geometry surrounding it.

Table 3: The seven model parameters considered in the influence analysis, all Arrhenius pre-exponential factors (see Table 1), with optimal values resulting from optimisation against the complete data set.

Idx.	Param.	Opt. value	Unit	Phase	Role
1	$A_{1,LP}$	2.87×10^{12}			Low-pressure limit of reaction #1
2	$A_{2,LP}$	2.11×10^{35}			Low-pressure limit of reaction #2
3	$A_{3,LP}$	4.90×10^{39}	cm ³ /mol/s	Gas	Low-pressure limit of reaction #3
4	$A_{5,LP}$	2.98×10^{68}			Low-pressure limit of reaction #5
5	$A_{8,rev}$	1.48×10^{14}			Reverse of reaction #8
6	A_{SR,SiH_4}	4.47×10^{33}	cm/mol/s	Particle	Surface reac.: silane addition, H ₂ -release
7	A_{H_2}	1.88×10^{18}	1/s		H ₂ -release from particle

Here, seven parameters were adjusted which represent key gas-phase and heterogeneous growth rates identified through sensitivity analysis [1]. We

1
2
3
4
5
6
7
8
9 note that this choice is consistent with reports in the literature [15] which
10 suggest that it is the low-pressure limit that is of interest to the conditions
11 considered in this work. Details are given in Table 3. Thus, the vector of
12 model parameters to be optimised is given by
13
14

$$\vartheta = (A_{1,LP}, A_{2,LP}, A_{3,LP}, A_{5,LP}, A_{8,rev}, A_{SR,SiH_4}, A_{H_2}).$$

15
16
17
18
19
20 The optimal values for the parameters resulting from optimisation against
21 the full data set are also given in Table 3. The differences in these values as
22 compared to [1] and [20] are due to the fact that different sets of responses
23 are being considered.
24
25
26

27 For the optimisation against the complete data set, 800 Sobol points were
28 generated, followed by 240 SPSA points. Recall that each point involves one
29 evaluation of the objective function (Eqn. 1), and that every objective func-
30 tion evaluation involves 19 model evaluations. For all subsequent optimisa-
31 tions, *i.e.* those of Φ_{-i} (Eqn. 3) with $i = 1, \dots, 19$, the model evaluations
32 performed as part of the original set of Sobol points can be re-used, as all
33 that is required is for each i to calculate the different objective function Φ_{-i}
34 for all of the points. For each of the Φ_{-i} optimisations, 120 SPSA points were
35 used. In total, this corresponds to about 3300 CPU-hours of computation.
36
37
38
39
40
41
42
43
44

45 The Cook distance analysis was conducted for all of the 19 experiments
46 in Table 2, and results are shown in Fig. 1. In this figure, the responses
47 are grouped by the particular experimental papers from which they were ob-
48 tained. Both of the two outlier thresholds, Eqn. (9) and Eqn. (10), are shown.
49 While several of the observations exceed the lower threshold (9), only two of
50 them exceed the upper one (10) (with one of them only marginally). This
51 is consistent with reports that (9) is too conservative in that it has a ten-
52
53
54
55
56
57
58
59
60
61
62
63
64
65

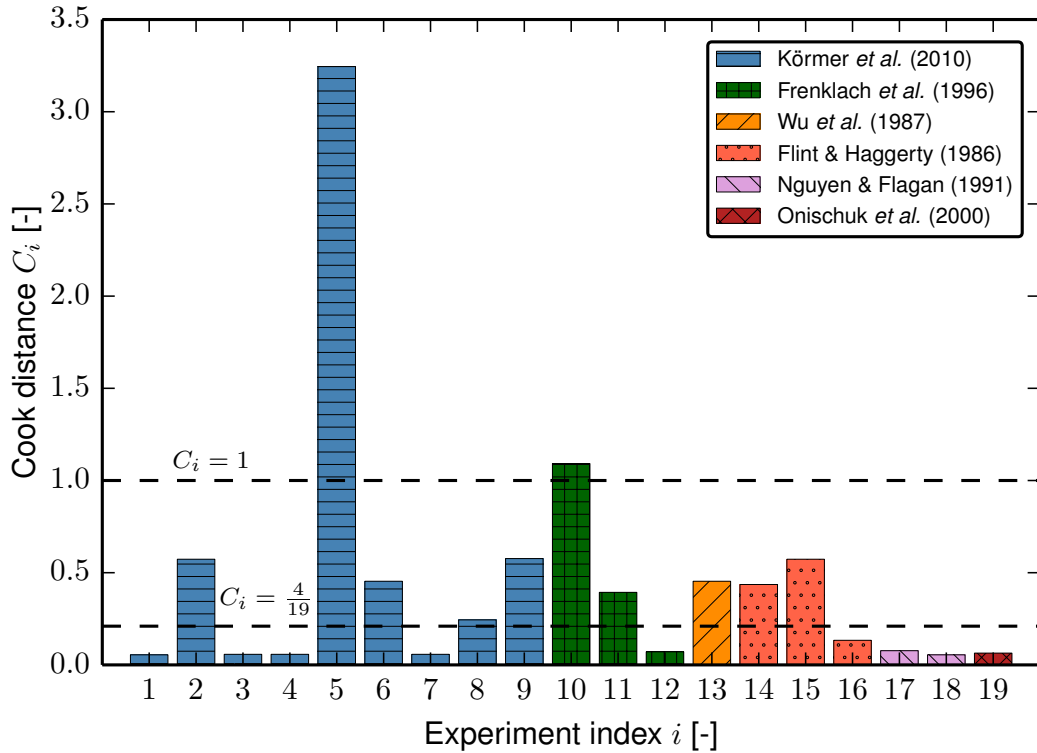
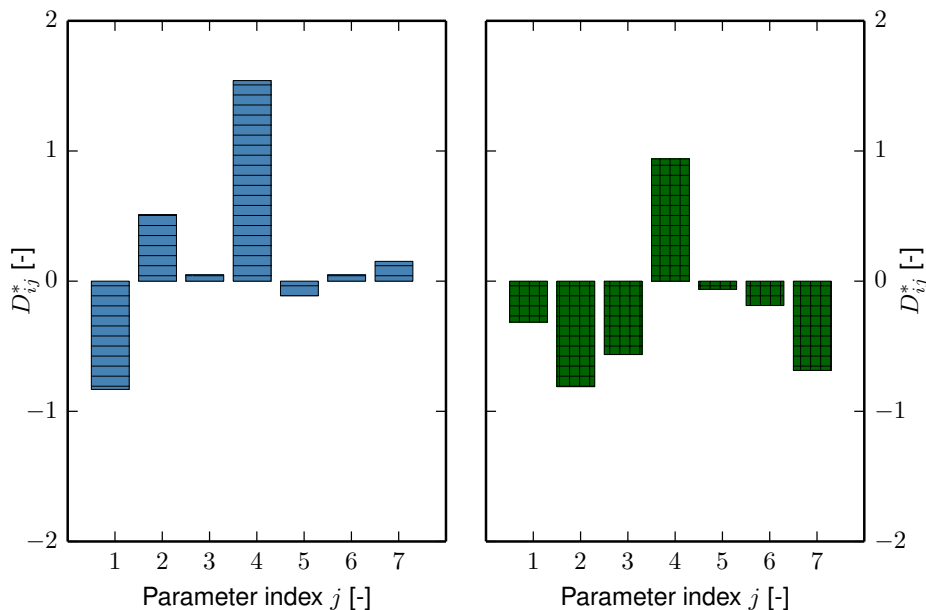


Figure 1: Overall influence of each of the experimental observations in Table 2 as measured by Cook's distance C_i (Eqn. 6). Each of the thresholds (9) and (10) are indicated through dashed horizontal lines.

dency to highlight too many observations, as mentioned in subsection 2.2.3. We conclude that observation $i = 5$ requires further attention, as its Cook distance exceeds both thresholds and is significantly larger than all the others. This indicates that this experimental point most strongly affects the objective function Φ (Eqn. 1), which in turn affects the parameter estimates, *i.e.* the optimal values $\hat{\vartheta}$ of the parameters (Eqn. 2). It could furthermore suggest that this particular observation might be an outlier with respect to the present model, or, more likely, that the model describes it inadequately.



(a) Influence of observation $i = 5$ by Körmer et al. [33] on each of the considered model parameters. (b) Influence of observation $i = 10$ by Frenklach et al. [34] on each of the considered model parameters.

Figure 2: DFBETA D_{ij}^* (Eqn. 5), for the two most influential experimental observations as identified in Fig. 1 (see also Table 2), for each of the parameters in Table 3.

Additionally, a DFBETA analysis was conducted to assess how the experimental observations affect the values of the parameters which are determined through the optimisation (Fig. 2). In terms of highlighting individual observations, the DFBETA analysis agrees with the Cook distance analysis: The values of D_{ij}^* for $i = 5$ and $i = 10$ are at least two orders of magnitude larger than those obtained for any other experiment. The DFBETA values for these experiments are shown in Figs. 2a and 2b respectively. We notice that the best estimate of parameter 4, *i.e.* the pre-exponential factor in the low-pressure limit of reaction 5 (Table 1), is influenced most by both of the

1
2
3
4
5
6
7
8
9 considered experimental observations.

10
11 In principle, there are two possible reasons for why an observation stands
12 out in a Cook distance or DFBETA analysis: errors associated with the ex-
13 periments, and errors associated with the model. Regarding experimental
14 errors, we assume here that all experimental data are both correct and ac-
15 curate. Considering model errors, these can be further categorised into the
16 following: errors arising from the solution methodology, *i.e.* numerical algo-
17 rithms, and flaws in the model. Specifically in this case, the latter include
18 reactor model errors, and deficiencies in the gas or particulate phase sub-
19 models.
20
21

22
23
24
25
26
27
28 Figure 3 shows particle size distributions for those experiments in Table 2
29 for which they have been measured. Two sets of model results are shown –
30 one for the optimisation against the complete data set, and one for the data
31 set with the 5th experiment omitted. As expected, if the 5th experiment
32 is omitted, the corresponding response deteriorates significantly (Fig. 3e).
33 Recall that only the means or modes of the distributions are optimised, not
34 the widths or any other characteristic. This is most obvious in cases 7-
35 9 (Figs. 3g-i) for example, where the modes agree reasonably well but the
36 model distributions are noticeably wider than the experimental ones. Note,
37 however, that adding, say, the standard deviation of the distributions as
38 optimisation targets by itself, *i.e.* without adding further degrees of freedom
39 in terms of model parameters to be optimised, will not ‘improve’ the fit in
40 any way. The fit can only improve if model parameters are included in the
41 optimisation which are suitable in the sense that they affect the width of the
42 distributions independently of the mean, provided such degrees of freedom
43
44
45
46
47
48
49
50
51
52
53
54
55
56
57
58
59
60
61
62
63
64
65

1
2
3
4
5
6
7
8
9
10
11
12
13
14
15
16
17
18
19
20
21
22
23
24
25
26
27
28
29
30
31
32
33
34
35
36
37
38
39
40
41
42
43
44
45
46
47
48
49
50
51
52
53
54
55
56
57
58
59
60
61
62
63
64
65

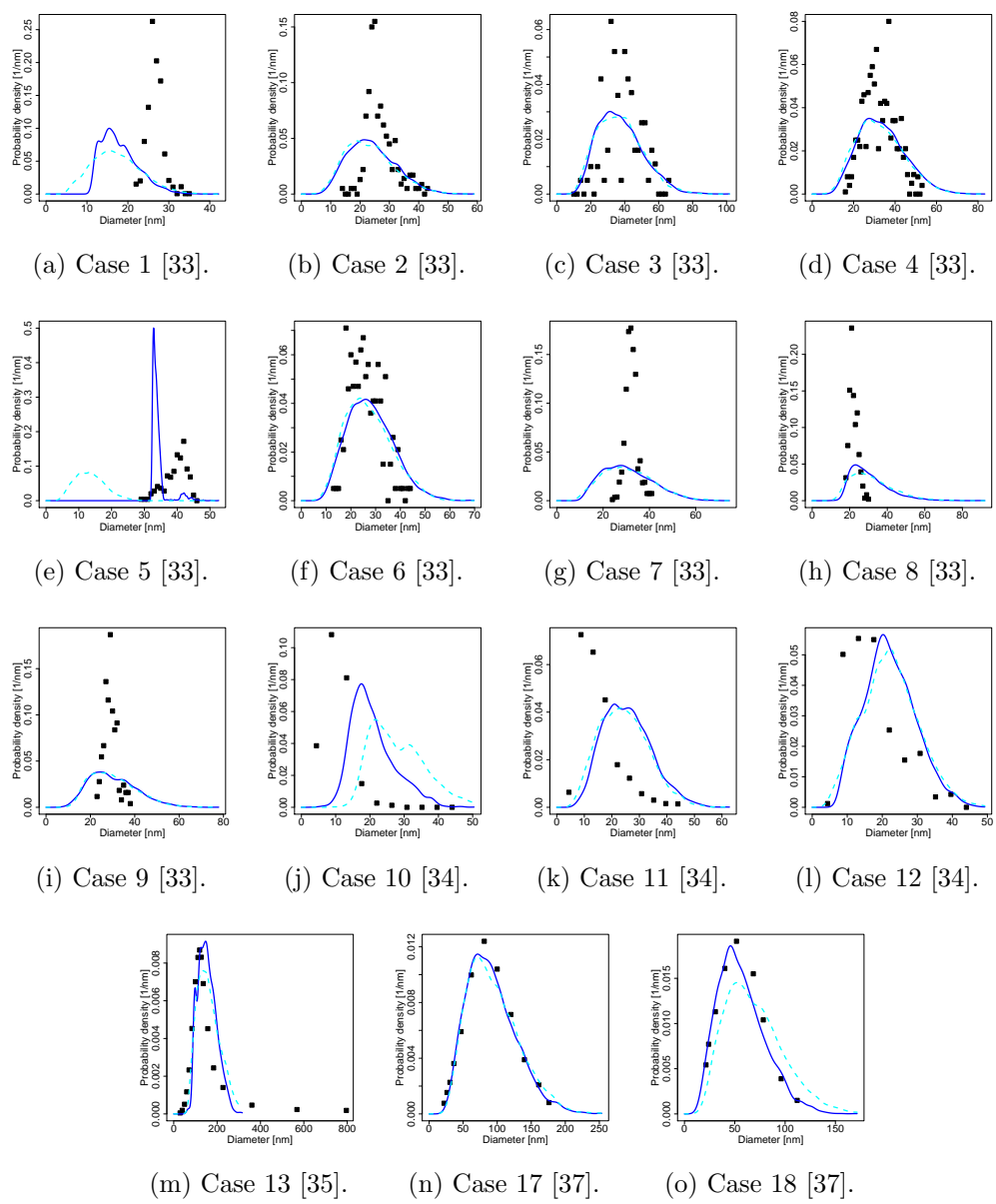


Figure 3: Particle size distributions for those experiments for which they were measured. Solid lines: model optimised against the complete data set. Dashed lines: model optimised against the data set with the 5th experiment omitted. Points: experiment.

1
2
3
4
5
6
7
8
9 exist in the model.

10
11 The $i = 5$ experiment refers to the case of lowest initial silane concen-
12 tration (0.5 mbar partial pressure) reported by Körmer et al. [33]. In this
13 hot-wall reactor experiment, a modal size of 41 nm was obtained for the pri-
14 mary particles, larger than that obtained for higher concentrations: 1 mbar
15 partial pressure yielded 27 nm primaries, 2 mbar yielded 24 nm primaries,
16 rising again to 31 nm at 4 mbar, all at the same residence time (and total
17 pressure). This inverse relationship for the smaller initial concentrations is
18 not captured by the model, thus indicating that this aspect requires fur-
19 ther development. More specifically, this suggests that the ratio between
20 the inception and condensation rates should be revisited, as this directly
21 controls the size and number of primary particles. Given that the incep-
22 tion mechanism in particular remains an active area of research, with several
23 fundamental open questions, this might be the most natural starting point.
24
25

26
27 In order to investigate further the kinetic role of initial silane concentra-
28 tion and total pressure, we conducted flux analyses of Si, time-integrated as
29 well as instantaneous, for a range of concentrations and pressures, covering
30 the conditions of all experiments in Table 2. At high dilutions, the impor-
31 tance of unimolecular reactions is expected to increase relative to bimolecular
32 ones. However, we found that, for the mechanism used, whilst the pressure
33 dependence of the net fluxes can be significant, their dependence on dilu-
34 tion is relatively minor within the range considered. Besides, we note that
35 even though experiment 5 is the most dilute amongst the ones by Körmer
36 et al. [33], experiments 13, 16, 17, and 18 are more dilute, some significantly
37 so (case 18 by a factor of 50), with the model agreeing well especially with
38
39
40
41
42
43
44
45
46
47
48
49
50
51
52
53
54
55
56
57
58
59
60
61
62
63
64
65

1
2
3
4
5
6
7
8
9
10
11
12
13
14
15
16
17
18
19
20
21
22
23
24
25
26
27
28
29
30
31
32
33
34
35
36
37
38
39
40
41
42
43
44
45
46
47
48
49
50
51
52
53
54
55
56
57
58
59
60
61
62
63
64
65

the latter three. Therefore, irrespective of the performance of the gas-phase mechanism at low silane concentrations, this alone is insufficient to explain the overall model behaviour for experiment 5.

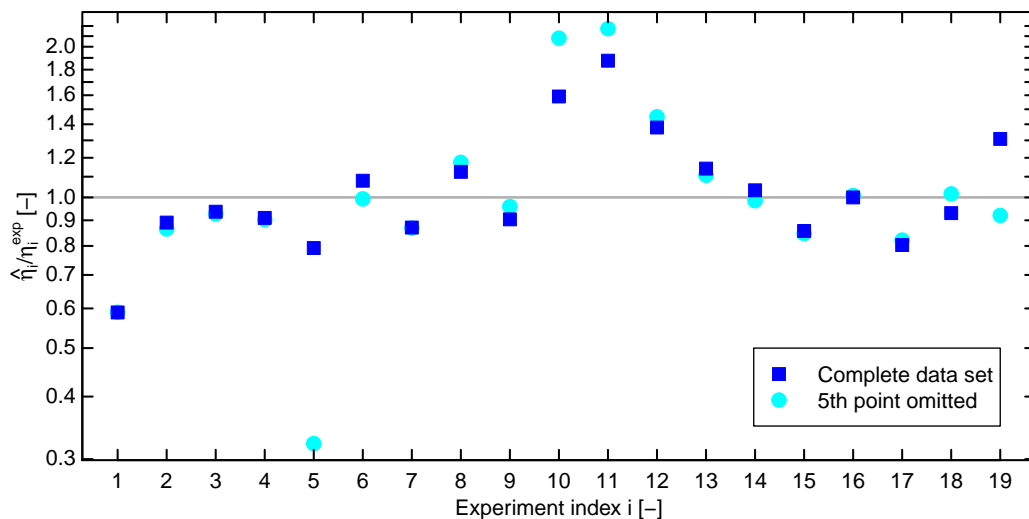


Figure 4: Ratios of model responses to experimental values for each of the 19 experiments in Table 2. Squares: model optimised against the complete data set. Circles: model optimised against the data set with the 5th experiment omitted.

Figure 4 shows ratios of model responses to experimental ones for all experiments. Again, two sets of results are shown – one for the optimisation against the complete data set, and one for the data set with the 5th experiment omitted, and the most obvious feature is again the worsening of the response corresponding to the 5th experiment. Even though some responses, such as for cases 10 and 11 (Figs. 3j and k), have deteriorated, one should note that the value of the overall objective function (Eqn. 3) is still lower for the omitted set than the full set. This is mainly due to responses 18 and 19, and also 13, improving and their absolute values being much larger

1
2
3
4
5
6
7
8
9 than those of responses 10 and 11. Referring again to Table 2, this hints
10 at a competition or trade-off between two very different scenarios which the
11 model is not capable of capturing simultaneously: the short residence-time
12 regime with early, nucleation-stage particles, versus the longer residence-time
13 regime with mature, larger aggregates.
14
15
16
17
18

19 **5. Conclusions**

20
21
22
23 We determined optimal values of seven parameters in a population bal-
24 ance model for the formation of silicon nanoparticles by means of least-
25 squares optimisation against a set of 19 experiments. The influence of each of
26 those measurements on the values of the considered kinetic model parameters
27 was then quantified using Cook’s distance and DFBETA – two basic omission-
28 based measures popular in the field of regression influence diagnostics. An
29 outlier analysis was then conducted by applying standard thresholds in or-
30 der to identify the most important experimental datasets in the optimisation.
31
32 This highlighted one particular experimental condition for further scrutiny.
33
34 We emphasise again that, in general, a particular measurement exceeding
35 an outlier threshold does not necessarily imply that there is a problem with
36 that measurement or more generally the experiment. In the first instance,
37 one should thoroughly examine whether there are shortcomings in the model
38 which are responsible for the disagreement with the measurement. This in-
39 forms future model development [57] by helping to identify aspects of the
40 model which require improvement. Furthermore, if one regards the model as
41 a formal representation of the best current knowledge about the experiment
42 or system under consideration [61], then the methods can be thought of as
43
44
45
46
47
48
49
50
51
52
53
54
55
56
57
58
59
60
61
62
63
64
65

1
2
3
4
5
6
7
8
9 giving an indication as to which measurements are most informative.
10
11

12 **Acknowledgements**

13
14
15 This work was partly funded by the Cambridge Australia Trust, by the
16 National Research Foundation (NRF), Prime Minister’s Office, Singapore un-
17 der its Campus for Research Excellence and Technological Enterprise (CRE-
18 ATE) programme, and by the European Union Horizon 2020 Research and
19 Innovation Programme under grant agreement 646121.
20
21
22
23
24
25

26 **References**

- 27
28
29 [1] W. J. Menz, M. Kraft, A new model for silicon nanopar-
30 ticle synthesis, *Combust. Flame* 160 (2013) 947–958.
31 doi:10.1016/j.combustflame.2013.01.014.
32
33
34
35 [2] S. Mosbach, M. Kraft, Influence of experimental observations on n-
36 propylbenzene kinetic parameter estimates, *Proc. Combust. Inst.* 35
37 (2015) 357–365. doi:10.1016/j.proci.2014.05.061.
38
39
40
41 [3] R. D. Cook, S. Weisberg, *Residuals and Influence in Regression*, Chap-
42 man and Hall, New York, 1982.
43
44
45
46 [4] R. Schall, T. T. Dunne, Influential variables in linear regression, *Tech-*
47 *nometrics* 32 (1990) 323–330. doi:10.1080/00401706.1990.10484685.
48
49
50
51 [5] R. D. Cook, Detection of influential observation in linear regression,
52 *Technometrics* 19 (1977) 15–18.
53
54
55
56
57
58

- 1
2
3
4
5
6
7
8
9 [6] N. R. Draper, J. A. John, Influential observations and
10 outliers in regression, *Technometrics* 23 (1981) 21–26.
11 doi:10.1080/00401706.1981.10486232.
12
13
14
15 [7] S. Chatterjee, A. S. Hadi, Influential observations, high leverage
16 points, and outliers in linear regression, *Stat. Sci.* 1 (1986) 379–393.
17 doi:10.1214/ss/1177013622.
18
19
20
21
22 [8] A. S. Tomlin, The role of sensitivity and uncertainty analysis
23 in combustion modelling, *Proc. Combust. Inst.* 34 (2013) 159–176.
24 doi:10.1016/j.proci.2012.07.043.
25
26
27
28 [9] R. Feeley, P. Seiler, A. Packard, M. Frenklach, Consistency of
29 a reaction dataset, *J. Phys. Chem. A* 108 (2004) 9573–9583.
30 doi:10.1021/jp047524w.
31
32
33
34
35 [10] A. V. Fiacco, G. P. McCormick, *Nonlinear Programming – Sequential*
36 *Unconstrained Minimization Techniques*, Classics in Applied Mathemat-
37 ics, SIAM, 1990.
38
39
40
41
42 [11] L. Eno, J. G. B. Beumee, H. Rabitz, Sensitivity analysis of experimen-
43 tal data, *Appl. Math. Comput.* 16 (1985) 153–163. doi:10.1016/0096-
44 3003(85)90005-0.
45
46
47
48 [12] H. Rabitz, M. Kramer, D. Dacol, Sensitivity analysis in chem-
49 ical kinetics, *Annu. Rev. Phys. Chem.* 34 (1983) 419–461.
50 doi:10.1146/annurev.pc.34.100183.002223.
51
52
53
54
55 [13] T. Turányi, Sensitivity analysis of complex kinetic systems.
56
57
58

1
2
3
4
5
6
7
8
9 Tools and applications, *J. Math. Chem.* 5 (1990) 203–248.
10 doi:10.1007/BF01166355.
11

12
13
14 [14] P. Ho, M. E. Coltrin, W. G. Breiland, Laser-induced fluorescence mea-
15 surements and kinetic analysis of Si atom formation in a rotating disk
16 chemical vapor deposition reactor, *J. Phys. Chem.* 98 (1994) 10138–
17 10147. doi:10.1021/j100091a032.
18
19

20
21
22 [15] E. L. Petersen, M. W. Crofton, Measurements of high-temperature silane
23 pyrolysis using SiH₄ IR emission and SiH₂ laser absorption, *J. Phys.*
24 *Chem. A* 107 (2003) 10988–10995. doi:10.1021/jp0302663.
25
26

27
28 [16] W. J. Menz, S. Shekar, G. P. E. Brownbridge, S. Mosbach, R. Körmer,
29 W. Peukert, M. Kraft, Synthesis of silicon nanoparticles with a narrow
30 size distribution: A theoretical study, *J. Aerosol Sci.* 44 (2012) 46–61.
31 doi:10.1016/j.jaerosci.2011.10.005.
32
33

34
35 [17] S. Shekar, A. J. Smith, W. J. Menz, M. Sander, M. Kraft, A
36 multidimensional population balance model to describe the aerosol
37 synthesis of silica nanoparticles, *J. Aerosol Sci.* 44 (2012) 83–98.
38 doi:10.1016/j.jaerosci.2011.09.004.
39
40

41
42 [18] S. Shekar, W. J. Menz, A. J. Smith, M. Kraft, W. Wagner, On a multi-
43 variate population balance model to describe the structure and compo-
44 sition of silica nanoparticles, *Comput. Chem. Eng.* 43 (2012) 130–147.
45 doi:10.1016/j.compchemeng.2012.04.010.
46
47

48
49 [19] W. J. Menz, R. I. A. Patterson, W. Wagner, M. Kraft, Ap-
50 plication of stochastic weighted algorithms to a multidimensional
51
52
53

1
2
3
4
5
6
7
8
9 silica particle model, *J. Comput. Phys.* 248 (2013) 221–234.
10 doi:10.1016/j.jcp.2013.04.010.
11

12
13
14 [20] W. J. Menz, G. P. E. Brownbridge, M. Kraft, Global sensitivity analysis
15 of a model for silicon nanoparticle synthesis, *J. Aerosol Sci.* 76 (2014)
16 188–199. doi:10.1016/j.jaerosci.2014.06.011.
17
18

19
20 [21] E. K. Y. Yapp, D. Chen, J. W. J. Akroyd, S. Mosbach,
21 M. Kraft, J. Camacho, H. Wang, Numerical simulation and para-
22 metric sensitivity study of particle size distributions in a burner-
23 stabilised stagnation flame, *Combust. Flame* 162 (2015) 2569–2581.
24 doi:10.1016/j.combustflame.2015.03.006.
25
26
27
28

29
30 [22] A. Kazakov, M. Frenklach, Dynamic modeling of soot particle coagula-
31 tion and aggregation: Implementation with the method of moments and
32 application to high-pressure laminar premixed flames, *Combust. Flame*
33 114 (1998) 484–501. doi:10.1016/S0010-2180(97)00322-2.
34
35
36
37

38
39 [23] D. A. Belsley, E. Kuh, R. E. Welsch, *Regression Diagnostics : Identifying*
40 *Influential Data and Sources of Collinearity*, John Wiley & Sons, 1980.
41
42

43 [24] R. D. Cook, S. Weisberg, Characterizations of an empirical influence
44 function for detecting influential cases in regression, *Technometrics* 22
45 (1980) 495–508. doi:10.1080/00401706.1980.10486199.
46
47
48

49 [25] N. R. Draper, H. Smith, *Applied Regression Analysis*, 2nd ed., John
50 Wiley & Sons, New York, 1981.
51
52

53
54 [26] M. Frenklach, in: W. C. Gardiner (Ed.), *Combustion Chemistry*,
55 Springer Verlag, New York, 1984, pp. 423–453.
56
57
58

- 1
2
3
4
5
6
7
8
9 [27] R. D. Cook, Influential observations in linear regression, *J. Am. Stat.*
10 *Assoc.* 74 (1979) 169–174.
11
12
13
14 [28] D. M. Bates, D. G. Watts, Relative curvature measures of nonlinearity,
15 *J. Roy. Stat. Soc. B* 42 (1980) 1–25.
16
17
18 [29] G. A. F. Seber, C. J. Wild, *Nonlinear Regression*, John Wiley & Sons,
19 2003.
20
21
22
23 [30] A. V. Fiacco, *Introduction to Sensitivity and Stability Analysis in Non-*
24 *linear Programming*, volume 165 of *Mathematics in Science and Engi-*
25 *neering*, Academic Press, New York, 1983.
26
27
28
29 [31] K. A. Bollen, R. W. Jackman, in: J. Fox, J. S. Long (Eds.), *Modern*
30 *Methods of Data Analysis*, Sage Publications, Newbury Park, 1990, pp.
31 257–291.
32
33
34
35
36 [32] R. D. Cook, S. Weisberg, in: S. Leinhardt (Ed.), *Sociological Methodol-*
37 *ogy*, Jossey-Bass, San Francisco, 1982, pp. 313–316.
38
39
40
41 [33] R. Körmer, M. P. M. Jank, H. Ryssel, H.-J. Schmid, W. Peukert, Aerosol
42 synthesis of silicon nanoparticles with narrow size distribution – Part
43 1: Experimental investigations, *J. Aerosol Sci.* 41 (2010) 998–1007.
44 doi:10.1016/j.jaerosci.2010.05.007.
45
46
47
48
49 [34] M. Frenklach, L. Ting, H. Wang, M. J. Rabinowitz, Silicon particle
50 formation in pyrolysis of silane and disilane, *Israel J. Chem.* 36 (1996)
51 293–303. doi:10.1002/ijch.199600041.
52
53
54
55
56
57
58
59
60
61
62
63
64
65

1
2
3
4
5
6
7
8
9
10
11
12
13
14
15
16
17
18
19
20
21
22
23
24
25
26
27
28
29
30
31
32
33
34
35
36
37
38
39
40
41
42
43
44
45
46
47
48
49
50
51
52
53
54
55
56
57
58
59
60
61
62
63
64
65

[35] J. J. Wu, H. V. Nguyen, R. C. Flagan, A method for the synthesis of sub-micron particles, *Langmuir* 3 (1987) 266–271. doi:10.1021/la00074a021.

[36] J. H. Flint, R. A. Marra, J. S. Haggerty, Powder temperature, size, and number density in laser-driven reactions, *Aerosol Sci. Tech.* 5 (1986) 249–260. doi:10.1080/02786828608959091.

[37] H. V. Nguyen, R. C. Flagan, Particle formation and growth in single-stage aerosol reactors, *Langmuir* 7 (1991) 1807–1814. doi:10.1021/la00056a038.

[38] A. A. Onischuk, A. I. Levykin, V. P. Strunin, K. K. Sabelfeld, V. N. Panfilov, Aggregate formation under homogeneous silane thermal decomposition, *J. Aerosol Sci.* 31 (2000) 1263–1281. doi:10.1016/S0021-8502(00)00031-8.

[39] H. Wiggers, R. Starke, P. Roth, Silicon particle formation by pyrolysis of silane in a hot wall gasphase reactor, *Chem. Eng. Technol.* 24 (2001) 261–264. doi:10.1002/1521-4125(200103)24:3<261::AID-CEAT261>3.0.CO;2-K.

[40] A. A. Onischuk, V. P. Strunin, M. A. Ushakova, V. N. Panfilov, Studying of silane thermal decomposition mechanism, *Int. J. Chem. Kinet.* 30 (1998) 99–110. doi:10.1002/(SICI)1097-4601(1998)30:2<99::AID-KIN1>3.0.CO;2-O.

[41] J. O. Odden, P. K. Egeberg, A. Kjekshus, From monosilane to crystalline silicon, part I: Decomposition of monosilane at 690-830 K and initial

1
2
3
4
5
6
7
8
9 pressures 0.1-6.6 MPa in a free-space reactor, *Solar Energy Materials*
10 *and Solar Cells* 86 (2005) 165–176. doi:10.1016/j.solmat.2004.07.002.
11
12

13
14 [42] J. O. Odden, P. K. Egeberg, A. Kjekshus, From monosilane to crys-
15 talline silicon, part II: Kinetic considerations on thermal decomposi-
16 tion of pressurized monosilane, *Int. J. Chem. Kinet.* 38 (2006) 309–321.
17 doi:10.1002/kin.20164.
18
19

20
21
22 [43] B. Giesen, H. Wiggers, A. Kowalik, P. Roth, Formation of Si-
23 nanoparticles in a microwave reactor: Comparison between experiments
24 and modelling, *Nanopart. Res.* 7 (2005) 29–41. doi:10.1007/s11051-005-
25 0316-z.
26
27
28

29
30
31 [44] J. Knipping, H. Wiggers, B. Rellinghaus, P. Roth, D. Konjhodzic,
32 C. Meier, Synthesis of high purity silicon nanoparticles in a low pres-
33 sure microwave reactor, *J. Nanosci. Nanotechnol.* 4 (2004) 1039–1044.
34 doi:10.1166/jnn.2004.149.
35
36
37

38
39 [45] A. Gupta, H. Wiggers, Surface chemistry and photoluminescence prop-
40 erty of functionalized silicon nanoparticles, *Physica E* 41 (2009) 1010–
41 1014. doi:10.1016/j.physe.2008.08.033.
42
43
44

45
46 [46] Z. Shen, T. Kim, U. Kortshagen, P. H. McMurry, S. A. Campbell, For-
47 mation of highly uniform silicon nanoparticles in high density silane
48 plasmas, *J. Appl. Phys.* 94 (2003) 2277–2283. doi:10.1063/1.1591412.
49
50
51

52
53 [47] N. J. Kramer, R. J. Anthony, M. Mamunuru, E. S. Aydil, U. R. Kortsha-
54 gen, Plasma-induced crystallization of silicon nanoparticles, *J. Phys. D*
55 47 (2014) 075202. doi:10.1088/0022-3727/47/7/075202.
56
57
58

1
2
3
4
5
6
7
8
9
10
11
12
13
14
15
16
17
18
19
20
21
22
23
24
25
26
27
28
29
30
31
32
33
34
35
36
37
38
39
40
41
42
43
44
45
46
47
48
49
50
51
52
53
54
55
56
57
58
59
60
61
62
63
64
65

[48] R. Körmer, H.-J. Schmid, W. Peukert, Aerosol synthesis of silicon nanoparticles with narrow size distribution – Part 2: Theoretical analysis of the formation mechanism, *J. Aerosol Sci.* 41 (2010) 1008–1019. doi:10.1016/j.jaerosci.2010.08.002.

[49] M. Gröschel, R. Körmer, M. Walther, G. Leugering, W. Peukert, Process control strategies for the gas phase synthesis of silicon nanoparticles, *Chem. Eng. Sci.* 73 (2012) 181–194. doi:10.1016/j.ces.2012.01.035.

[50] W. R. Cannon, S. C. Danforth, J. S. Flint, J. S. Haggerty, R. A. Marra, Sinterable ceramic powders from laser-driven reactions: I, Process description and modeling, *J. Am. Ceram. Soc.* 65 (1982) 324–330. doi:10.1111/j.1151-2916.1982.tb10464.x.

[51] W. R. Cannon, S. C. Danforth, J. S. Haggerty, R. A. Marra, Sinterable ceramic powders from laser-driven reactions: II, Powder characteristics and process variables, *J. Am. Ceram. Soc.* 65 (1982) 330–335. doi:10.1111/j.1151-2916.1982.tb10465.x.

[52] J. Flint, J. Haggerty, A model for the growth of silicon particles from laser-heated gases, *Aerosol Sci. Tech.* 13 (1990) 72–84. doi:10.1080/02786829008959425.

[53] M. Meunier, J. H. Flint, J. S. Haggerty, D. Adler, Laser-induced chemical vapor deposition of hydrogenated amorphous silicon. I. Gas-phase process model, *J. Appl. Phys.* 62 (1987) 2812–2821. doi:10.1063/1.339412.

1
2
3
4
5
6
7
8
9
10
11
12
13
14
15
16
17
18
19
20
21
22
23
24
25
26
27
28
29
30
31
32
33
34
35
36
37
38
39
40
41
42
43
44
45
46
47
48
49
50
51
52
53
54
55
56
57
58
59
60
61
62
63
64
65

[54] M. Meunier, J. H. Flint, J. S. Haggerty, D. Adler, Laser-induced chemical vapor deposition of hydrogenated amorphous silicon. II. Film properties, *J. Appl. Phys.* 62 (1987) 2821–2829. doi:10.1063/1.339413.

[55] cmcl innovations, MoDS (Model Development Suite), version 0.2.3, 2015. <http://www.cmclinnovations.com/mod-suite/>.

[56] S. Mosbach, J. H. Hong, G. P. E. Brownbridge, M. Kraft, S. Gudiyella, K. Brezinsky, Bayesian error propagation for a kinetic model of n-propylbenzene oxidation in a shock tube, *Int. J. Chem. Kinet.* 46 (2014) 389–404. doi:10.1002/kin.20855.

[57] S. Mosbach, A. Braumann, P. L. W. Man, C. A. Kastner, G. P. E. Brownbridge, M. Kraft, Iterative improvement of Bayesian parameter estimates for an engine model by means of experimental design, *Combust. Flame* 159 (2012) 1303–1313. doi:10.1016/j.combustflame.2011.10.019.

[58] I. M. Sobol, On the systematic search in a hypercube, *SIAM J. Numer. Anal.* 16 (1979) 790–793.

[59] J. C. Spall, Implementation of the Simultaneous Perturbation Algorithm for stochastic optimization, *IEEE T. Aero. Elec. Sys.* 34 (1998) 817–823. doi:10.1109/7.705889.

[60] T. Hirokami, Y. Maeda, H. Tsukada, Parameter estimation using simultaneous perturbation stochastic approximation, *Electr. Eng. Jpn* 154 (2006) 30–39. doi:10.1002/ej.20239.

1
2
3
4
5
6
7
8
9
10
11
12
13
14
15
16
17
18
19
20
21
22
23
24
25
26
27
28
29
30
31
32
33
34
35
36
37
38
39
40
41
42
43
44
45
46
47
48
49
50
51
52
53
54
55
56
57
58
59
60
61
62
63
64
65

[61] M. Frenklach, Transforming data into knowledge – Process Informatics for combustion chemistry, *Proc. Combust. Inst.* 31 (2007) 125–140. doi:10.1016/j.proci.2006.08.121.

1
2
3
4
5
6
7
8
9
10
11
12
13
14
15
16
17
18
19
20
21
22
23
24
25
26
27
28
29
30
31
32
33
34
35
36
37
38
39
40
41
42
43
44
45
46
47
48
49
50
51
52
53
54
55
56
57
58
59
60
61
62
63
64
65

List of Figures

- 1 Overall influence of each of the experimental observations in Table 2 as measured by Cook’s distance C_i (Eqn. 6). Each of the thresholds (9) and (10) are indicated through dashed horizontal lines. 19
- 2 DFBETA D_{ij}^* (Eqn. 5), for the two most influential experimental observations as identified in Fig. 1 (see also Table 2), for each of the parameters in Table 3. 20
- 3 Particle size distributions for those experiments for which they were measured. Solid lines: model optimised against the complete data set. Dashed lines: model optimised against the data set with the 5th experiment omitted. Points: experiment. . . . 22
- 4 Ratios of model responses to experimental values for each of the 19 experiments in Table 2. Squares: model optimised against the complete data set. Circles: model optimised against the data set with the 5th experiment omitted. 24